



Performance Comparison of Serial and Parallel Hybrid Fiber Amplifier under Optimum Pump Conditions

Aseel A. Khudair^{a,*}, Abdulla K. Abass^b , Mudhafer H. Ali^c

^{a,b} Laser and Optoelectronic Engineering Dept., University of Technology-Iraq, Alsina'a Street, 10066 Baghdad, Iraq.

^c Computer Engineering Dept, College of Engineering, Al-Iraqia University, Baghdad, Iraq.

*Corresponding author Email: loe.19.05@grad.uotechnology.edu.iq

HIGHLIGHTS

- The performance parameters for both S- and P-HFOA were simulated and compared at OPP via OptiSystem software.
- The S-HFOA has a high average gain and an appropriate NF, but the gain bandwidth is limited.
- The P-HFOA has a wide 3-dB gain bandwidth and high saturation power as compared to the S-HFOA.

ABSTRACT

In this work, two different configurations of hybrid fiber optical amplifiers are investigated and simulated via OptiSystem 7.0 software, namely, serial and parallel hybrid fiber optical amplifiers (S- and P-HFOAs). The investigation involves performance comparison for the S- and P-HFOA under optimum pump conditions to demonstrate the advantages and disadvantages of each configuration. The simulation results show that the serial configuration has a high average gain level of 19.2 dB, an appropriate noise figure about 4.3 dB, but low saturation power, and limited gain bandwidth of approximately 40 nm, which is considered a primary issue in S-HFOA design, in addition to the pump conversion efficiency still insufficient in the Raman amplifier stage. While in P-HFOA design, a wide 3-dB gain bandwidth of more than 60 nm is maintained, along with an average gain level of 13.5 dB, high average noise figure about 8.3 dB and high saturation power due to the absent of cascading effect in parallel configuration.

ARTICLE INFO

Handling editor: Ivan A. Hashim

Keywords: Serial hybrid amplifier; Optimum pump power; Parallel hybrid amplifier

1. Introduction

The optical amplifier is an important component for compensating the transmission losses in the optical communication system [1]–[3]. One essential type of fiber optic amplifier employed by many researchers is an erbium-doped fiber amplifier (EDFA), which is emerged firstly in the first generation for covering the conventional communication band (C-band) with wavelengths ranging from 1530 nm to 1565 nm [4], [5]. The other type is the Raman fiber amplifier (RFA), which can provide gain at any wavelength within the transparency window of optical fiber by simply changing the pump wavelength [6]. Therefore, a fiber amplifier is upgraded to a hybrid fiber amplifier as a solution to the problem of consuming most of the applicable communication band (C-band), as the aim of HFOA is to expand the gain bandwidth by combining two or more amplifiers with different operating bands. In addition, to the other performance enhancing of the optical fiber amplifier, such as: increasing pump efficiency in terms of using a single pump unit with low pump power, and extending repeater distance.

In general, hybrid fiber optical amplifiers (HFOA) are classified according to the signal path. Clearly, when the amplification stages share the same signal path they will be configured as a serial hybrid fiber optic amplifier (S-HFOA). In contrast, if the signal is separated into two individual paths, it is configured as a parallel hybrid fiber optic amplifier (P-HFOA). Due to this different tracing of the signal, each configuration has its advantages and disadvantages. In the context, serial design is characterized by a high average gain level (G_{av}) and an appropriate noise figure (NF), but there is a limitation in gain bandwidth (GB), which is considered a primary issue in such configuration, furthermore the power conversion efficiency (PCE) is still insufficient in the RFA stage [7]–[10].

While, in parallel design the flatness gain bandwidth can be controlled by setting the signal ratio [11], [12]. In addition, to enhance the gain bandwidth of P-HFOA several approaches have been proposed utilizing the gain control [12], [13] and to solve the dispersion problem in the EDFA branch utilizing the combination between the serial and parallel hybrid fiber amplifiers

[14]–[16] in this combination, a second DCF is added to work as a gain medium for the RFA and to compensate the dispersion in the EDFA branch.

To the best of our knowledge, the performance parameters for both S– and P–HFOA were simulated and compared at optimum pump conditions via OptiSystem7.0 software for the first time. The optimum pump power is determined based on the literature, in which a higher average gain level, a wide gain spectrum, and the appropriate noise figure can be achieved. The research emphasized the critical role of comparison for different configurations of hybrid fiber amplifiers, which can be useful to designers when selecting the optimum amplifier structure for their work as it gives detailed performance parameters under optimum pump conditions.

2. Simulation Model

The schematic designs of both S– and P–HFOA are shown in Figure 1(a) and (b), respectively. These configurations consist of two stages. The first stage of these hybrid amplifiers is an EDFA amplifier, while the second stage is an RFA amplifier. Both architectures use backward-propagating pumping. The signal is provided by a continuous wave laser (CW) with a maximum power of 10 dBm, wavelength ranging from 1530 nm to 1600 nm, C+L band, and the line-width is 150 KHz. The length of EDFA is approximately 3 m. The doping radius is about $1.65 \mu\text{m}$, the core area of $1.65 \mu\text{m}^2$ and the doping concentration is about $1.4 \times 10^{25} \text{ m}^{-3}$. It is pumped at the wavelength's of 1480 nm with pump powers of 100 mW (residual Raman pump power). The second stage of the HFOA is composed of the Raman amplifier using a 7 km DCF with an effective area of $20 \mu\text{m}^2$ and an attenuation coefficient of 0.5 dB/km, at 1550 nm, dispersion coefficient of $-110 \text{ ps}/(\text{nm} \cdot \text{km})$. A wavelength selective coupler (WSC) is utilized to isolate the residual Raman pump from the reflected Rayleigh scattering signal. To record the overall system gain, an optical spectrum analyzer (OSA) is utilized. Finally, the output signal from the two branches is collected using an optical fiber coupler (OFC).

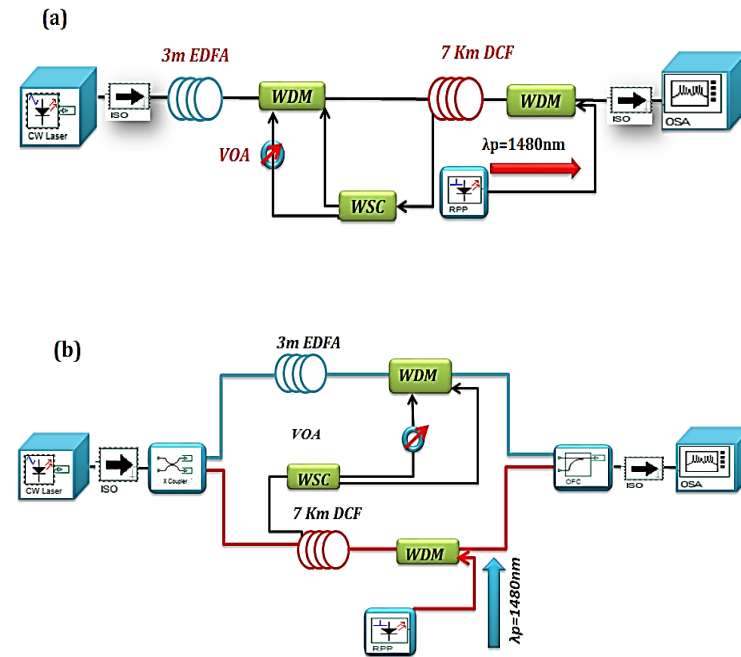


Figure 1: Schematic diagram for the proposed HFOA: (a) S–HFOA and (b) P–HFOA

3. Results and Discussion

This paper aims to compare the performance parameters of both S– and P–HFOA at the same design parameters except for pumping power that should be settled at its optimum conditions (OPP). The comparison covered several parameters such as; gain bandwidth (GB), average gain (G_{av}), average noise figure (NF_{av}), saturation power (P_{sat}), and pump conversion efficiency (PCE). The hybrid gain profile for both configurations at various signal regions is illustrated in Figure 2 (a) and (b). The input signal wavelength (λ_{in}) was swept from (1530 nm to 1600 nm), with 5 nm in steps, to achieve a gain spectrum at different input signal power values of -25 dBm and -10 dBm under optimum pump power and wavelength (600 mW for S–HFOA and 800 mW for P–HFOA at 1480 nm). Under a small signal region of -25 dBm , S–HFOA exhibits higher average gain and limited amplification bandwidth than P–HFOA. However, the overall average gain is about 19 dB and 13.5 dB, within 40 nm and 60 nm of amplification gain bandwidth, for S– and P–HFOA, respectively.

When P_{in} increased to -10 dBm , the bandwidth expanded to 45 nm and 65 nm, while the average gain level decreased to 16 dB and 11 dB for S– and P–HFOA, respectively. As shown in Figure 2 below, it is clear that the P–HFOA shows a gain bandwidth about 20 nm higher than the gain bandwidth of S–HFOA, which is attributed to the absence of a cascading effect between the

amplification stages in P-HFOA. The noise figure (NF) values of two different hybrid configurations versus the input wavelength at the input signal powers of -25 dBm and -10 dBm are depicted in Figure 3 (a) and (b). The NF of S-HFOA mainly depends on the first amplifier [7]. Definitely, low values of noise figure less than 5 dB are observed at small input signal power -25 dBm within the gain bandwidth. That is because the noise figure is more affected by the first amplifier stage, which is an EDFA in the S-HFOA configuration, in addition to the fact that no saturation could occur in EDFA. While, in P-HFOA, high noise figure values are observed at large input signal power -10 within the gain bandwidth because both amplifier stages, Er-DFA and RFA, suffered from saturation due to large input signal power, which reduced the gain and raised the noise level at the amplified signal. Under both input Power signals the proposed HFOA within the flat gain bandwidth shows an average NF of about 4.6 dB and 8.3 dB for S- and P-HFOA, respectively.

To complete this comparison, the saturation power of both hybrid amplifiers was investigated under two different input signal wavelengths, namely, 1530 nm and 1580 nm, to give an idea of the gain saturation effect on the gain spectra. The signal power varied from -25 dBm to 10 dBm with a step of 1 dBm. The P_{sat} is determined when the gain level is dropped 3 -dB from its constant or maximum value.

At 1530 nm, the gain was saturated at approximately -12 dBm for S-HFOA and -9 dBm for P-HFOA. For the reason that this wavelength, 1530 nm, falls within the conventional band region where the Er-DFA gain is more effective in comparison to the RFA gain, since the peak gain of the Raman amplifier is quite far from 1530 nm. Because of that, the gain saturation G_{sat} of an erbium amplifier has a significant impact on the overall gain saturation of the hybrid amplifier. Meanwhile, at 1580 nm, a broader gain dynamic range was observed, and the appearance of saturated power was delayed until -3 dBm for S-HFOA and to 1 dBm for P-HFOA. The results show that at various signal wavelengths, as illustrated in figure 4, the saturation in gain level occurs faster in S-HFOA than in P-HFOA due to the cascaded amplifier stage in S-HFOA. The analyzed data from Figures 2, 3 and 4 Summaries the performance parameters for both S-HFOA and P-HFOA under optimum pump conditions as depicted in Table 1.

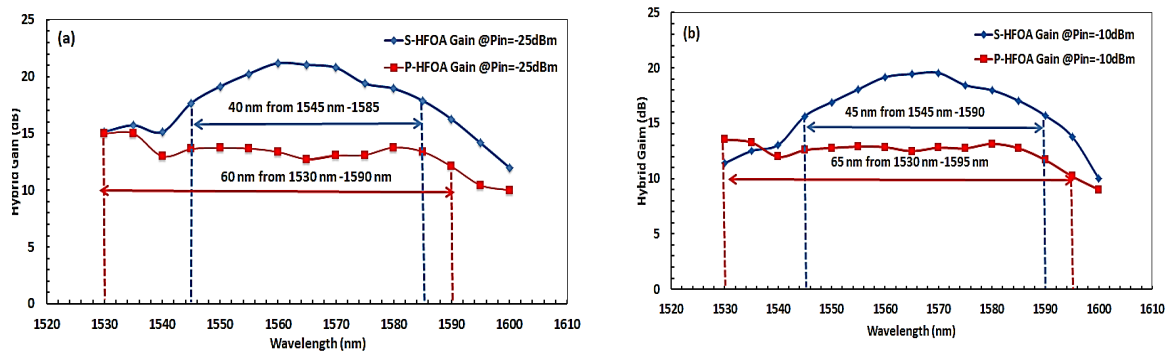


Figure 2: Hybrid gain profile of S- and P-HFOA at (a) small signal power -25 dBm and (b) large signal power -10 dBm

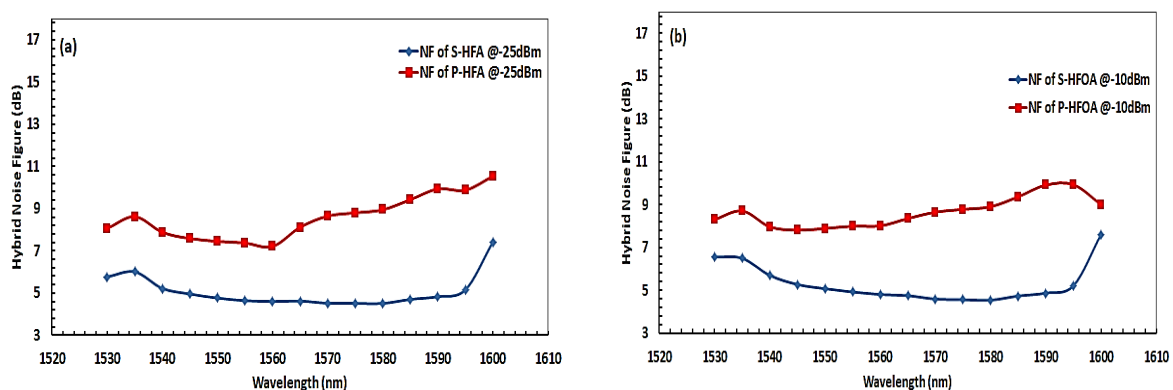


Figure 3: Hybrid NF versus input signal wavelengths of S- and P-HFOA at (a) small signal power -25 dBm and (b) large signal power -10 dBm.

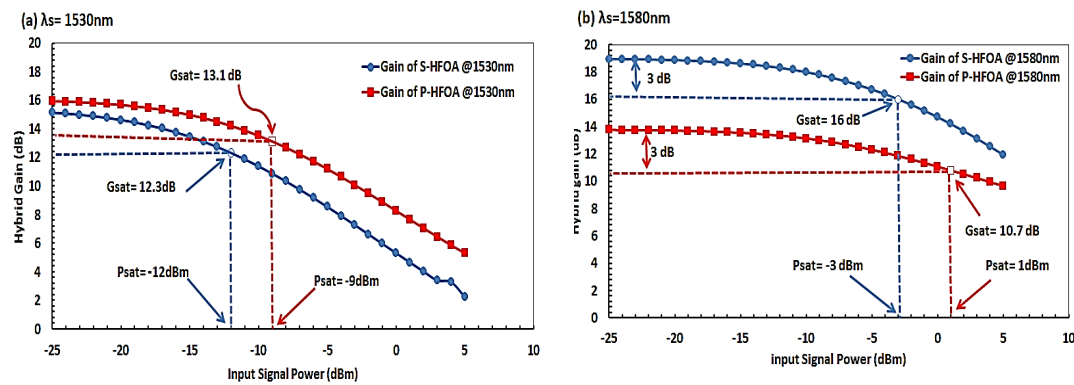


Figure 4: Hybrid Gain level against the input signal power for S-HFOA and P-HFOA under two different region of wavelengths: (a) 1530 nm, C-band and (b) 1580 nm, L-band.

Table 1: Summaries the performance parameters for both S-HFOA and P-HFOA under optimum pump conditions

| Structure | GB (dB) | Gav (dB) | NFav (dB) | PCE % (dB/mW) | Psat (dBm) | |
|-----------|---------|----------|-----------|---------------|------------|--------|
| | | | | | 1530nm | 1580nm |
| S-HFOA | 40 | 19.2 | 4.6 | 3.057 | -12 | -3 |
| P-HFOA | 60 | 13.5 | 8.3 | 1.802 | -9 | 1 |

4. Conclusion

The performance parameters for both S-HFOA and P-HFOA were investigated and compared under the same design parameters except the pump power selected to be at optimum pump conditions. According to the results, the S-HFOA has a high overall average gain level and an appropriate NF, but an issue in gain flatness still exists. In an RFA stage, pump conversion efficiency (PCE) remains insufficient. In contrast, P-HFOA has the highest saturation power and wide 3-dB gain bandwidth. This can be attributed to the effect of cascading amplification stage in S-HFOA and both amplifiers, shearing the same signal path in S-HFOA. Finally, this comparison can be useful to the designers when selecting the optimum amplifier structure for their work as it gives detailed performance parameters under optimum pump conditions.

Author contribution

All authors contributed equally to this work.

Funding

This research received no specific grant from any funding agency in the public, commercial, or not-for-profit sectors.

Data availability statement

The data that support the findings of this study are available on request from the corresponding author.

Conflicts of interest

The authors declare that there is no conflict of interest.

References

- [1] A. K. Abass, M. H. Al-Mansoori, M. Z. Jamaludin, F. Abdullah, T. F. Al-Mashhadani, Raman Amplification Effects on Stimulated Brillouin Scattering Threshold in Multiwavelength Brillouin-Raman Fiber Laser, *Int. Conf. Photo.*, (2012) 171–174. <http://dx.doi.org/10.1109/ICP.2012.6379832>
- [2] M. H. Ali, F. Abdullah, M. Z. Jamaludin, M. H. Al-Mansoori, A. Ismail, A. K. Abass, Simulation and Experimental Validation of Gain Saturation in Raman Fiber Amplifier, *Int. Conf. Photo.*, (2012) 27–29. <http://dx.doi.org/10.1109/ICP.2012.6379850>
- [3] A. A. Almukhtar, Flat-gain and wide-band partial double-pass erbium co-doped fiber amplifier with hybrid gain medium, *Opt. Fiber. Technol.*, 52 (2019) 101952. <http://dx.doi.org/10.1016/j.yofte.2019.101952>
- [4] A. K. Abass, M. J. Abdul-Razak, M. A. Salih, Gain Characteristics for C-Band Erbium Doped Fiber Amplifier Utilizing Single and Double-Pass Configurations: A Comparative Study, *Eng. Tech. J.*, 32 (2014) 2165–2173. <http://dx.doi.org/10.30684/ETJ.32.9A5>

- [5] M. H. Ali, A. H. Ali, S. M. Abdulsatar, M. A. Saleh, A. K. Abass, T. F. Al-Mashhadani, Pump power optimization for hybrid fiber amplifier utilizing second order stimulated Raman scattering, *Opt. Quantum. Electron.*, 52 (2020) 1–8. <https://doi.org/10.1007/s11082-020-02400-x>
- [6] C. H. G. Agrawal, *Raman Amplification in Fiber Optical Communication Systems*, USA Elsevier Acad., 33–97 (2005).
- [7] M. H. Ali, F. Abdullah, M. Z. Jamaludin, M. H. Al-Mansoori, A. K. Abass, T. F. Al-Mashhadani, Effect of Cascading Amplification Stages on the Performance of Serial Hybrid Fiber Amplifier, *Fiber. Integr. Opt.*, 34 (2015) 131-144 . <http://dx.doi.org/10.1080/01468030.2015.1061621>
- [8] M. H. Ali, A. K. Abass, M. A. Saleh, S. H. Alnajjar, Wideband serial hybrid fiber amplifier utilizing higher order stimulated Raman scattering, *Sci. Conf. Electr. Eng.*, (2018) 291–293. <http://dx.doi.org/10.1109/SCEE.2018.8684123>
- [9] F. Abdullah , M. Z. Jamaludin, Influence of Raman Pump Direction on the Performance of Serial Hybrid Fiber Amplifier in C + L-Band, *IEEE . Int. Conf. Photo.*, (2018)1–3. <http://dx.doi.org/10.1109/ICP.2018.8533180>
- [10] I. A. Gurkaynak, T. F. Al-Mashhadani, M. Yucel, H. H. Goktas, Broadly Flatness Gain Band with Double Pass-Serial Hybrid Optical Amplifier Utilizing Single Pump Unit, *Int. Conf. Electr. Electron. Eng.*, (2021) 32–35 . <http://dx.doi.org/10.1109/ICEEE52452.2021.9415958>
- [11] S. K. Liaw, C. K. Huang, Y. L. Hsiao, Parallel-type C+L band hybrid amplifier pumped by 1480 nm laser diodes, *Laser. Phys. Lett.*, 5 (2008) 543–546. <http://dx.doi.org/10.1002/lapl.200810029>
- [12] M. H. Ali, F. Abdullah, Z. Jamaludin, M. Hayder, Simulation and Experimental Validation of Gain-Control Parallel Hybrid Fiber Amplifier, 18 (2014) 657–662.
- [13] M. H. Ali, F. Abdullah, T. F. Al-Mashhadani, Gain-control technique in double-pass parallel hybrid fiber amplifier, *Opt. Quantum Electron.*, 52 (2020) 386. <http://dx.doi.org/10.1007/s11082-020-02508-0>
- [14] A. K. Abass, M. H. Ali, S. A. A. Al-Hussein, Optimization of Hybrid Fiber Amplifier Utilizing Combined Serial-Parallel Configuration, *IOP. Conf. Series. Mate. Sci. Eng.*, 454 (2018) 012014. <http://dx.doi.org/10.1088/1757-899X/454/1/012014>
- [15] M. H. Ali, A. K. Abass, S. A. Abd Al-Hussein, 32 Channel \times 40 Gb/s WDM optical communication system utilizing different configurations of hybrid fiber amplifier, *Opt. Quantum. Electron.*, 51 (2019) 188. <http://dx.doi.org/10.1007/s11082-019-1842-8>
- [16] A. K. Abass, M. H. Ali, S. A. A. Al-hussein, Wideband flat-gain hybrid fiber amplifier utilizing combined serial-parallel configuration, *Int. J. Nanoelectron. Mater.*, 11 (2018) 17–22.